Received: 12 November 2022 | Revised: 27 March 2023 | Accepted: 6 April 2023

DOI: 10.1111/cas.15822

ORIGINAL ARTICLE

Cancer Science WILEY

ANP32B suppresses B-cell acute lymphoblastic leukemia through activation of PU.1 in mice

Qian Yang[1] | Hao-Ran Liu[1] | Shuo Yang[2] | Yu-Sheng Wei[1] | Xiao-Na Zhu[3] | Zhe Zhi[3] | Di Zhu[3] | Guo-Qiang Chen[3] | Yun Yu[3]

[1]Key Laboratory of Cell Differentiation and Apoptosis of Chinese Ministry of Education, Rui-Jin Hospital, Shanghai Jiao-Tong University School of Medicine (SJTU-SM), Shanghai, China

[2]Department of Laboratory Medicine, Zhongshan Hospital, Fudan University, Shanghai, China

[3]Institute of Aging & Tissue Regeneration, State Key Laboratory of Oncogenes and Related Genes and Chinese Academy of Medical Sciences Research Unit (NO.2019RU043), Ren-Ji Hospital, Shanghai Jiao-Tong University School of Medicine (SJTU-SM), Shanghai, China

Correspondence
Yun Yu and Guo-Qiang Chen, 280, Chong-Qing South Road, Shanghai 200025, China.
Email: yy@shsmu.edu.cn and chengq@shsmu.edu.cn

Funding information
National Key R&D Program of China, Grant/Award Number: 2020YFA0803403; National Natural Science Foundation of China, Grant/Award Number: 82270156 and 91853206; CAMS Innovation Fund for Medical Sciences, Grant/Award Number: 2019-I2M-5-051; Shanghai Committee of Science and Technology, Grant/Award Number: 20JC1410100

Abstract

ANP32B, a member of the acidic leucine-rich nuclear phosphoprotein 32 kDa (ANP32) family of proteins, is critical for normal development because its constitutive knockout mice are perinatal lethal. It is also shown that ANP32B acts as a tumor-promoting gene in some kinds of cancer such as breast cancer and chronic myelogenous leukemia. Herein, we observe that ANP32B is lowly expressed in B-cell acute lymphoblastic leukemia (B-ALL) patients, which correlates with poor prognosis. Furthermore, we utilized the N-myc or BCR-ABL^{p190}-induced B-ALL mouse model to investigate the role of ANP32B in B-ALL development. Intriguingly, conditional deletion of *Anp32b* in hematopoietic cells significantly promotes leukemogenesis in two B-ALL mouse models. Mechanistically, ANP32B interacts with purine rich box-1 (PU.1) and enhances the transcriptional activity of PU.1 in B-ALL cells. Overexpression of PU.1 dramatically suppresses B-ALL progression, and highly expressed PU.1 significantly reverses the accelerated leukemogenesis in *Anp32b*-deficient mice. Collectively, our findings identify ANP32B as a suppressor gene and provide novel insight into B-ALL pathogenesis.

KEYWORDS
ANP32B, B-ALL, leukemogenesis, PU.1, tumor suppressor

Abbreviations: B-ALL, B-cell acute lymphoblastic leukemia; BCL6, B cell lymphoma 6; CCND1, recombinant cyclin d1; CCND2, recombinant cyclin d2; CML, chronic myelogenous leukemia; HDAC1, histone deacetylase 1; IRES, internal ribosome entry site; IRF7, interferon regulatory factor 7; KLF5, krüppel-like factor 5; PEST, polypeptide sequences enriched in proline, glutamate, serine, and threonine; PU.1, purine rich box-1; Q-pcr, quantitative real-time polymerase chain reaction; SMARCA5, SWI/SNF-related, matrix-associated, actin-dependent regulator of chromatin, subfamily A member 5; TAD, topologically associating domain; TSS, transcriptional start sites.

Qian Yang, Hao-Ran Liu, and Shuo Yang contributed equally to this work.

1 | INTRODUCTION

B-cell acute lymphoblastic leukemia (B-ALL) is a group of hematological malignancies caused by the clonal proliferation of lymphoid progenitor cells combined with a blockage of B-cell differentiation, which commonly occurs in children and also in adult populations.[1] The oncogenesis of B-ALL is often associated with various genetic lesions, including oncogenic fusions derived from chromosomal translocations such as *ETV6-RUNX1*, *BCR-ABL1*, or *TCF3-PBX1*.[2] These chromosomal aberrations are important in leukemia initiation, but they alone are insufficient to generate a full leukemic phenotype.[3] It has been discovered that the mutations or abnormal expressions of related genes involved in B-cell development, signal transduction, and epigenetic regulation play important roles in the development of B-ALL.[3–5] Despite advances in the treatment of B-ALL, including chemotherapy, bone marrow (BM) transplantation, chimeric antigen receptor T cell (CAR-T) immunotherapy, or combinations of these treatments,[6–8] 20% of child B-ALL patients still have treatment failure. The prognosis is even worse in adult B-ALL patients, as only 30% of them achieve long-term survival,[9,10] therefore novel therapeutic targets are urgently needed to treat B-ALL more effectively.

ANP32B belongs to the highly conserved acidic leucine-rich nuclear phosphoprotein 32 kDa (ANP32) family, whose members including ANP32A, B, and E, which is characterized by an N-terminal leucine-rich repeat domain and a C-terminal low-complexity acidic region.[11] Although the ANP32 proteins functionally overlap in a broad array of physiological processes, they have been reported to have diverse roles in cancer progression.[12] ANP32A is a putative tumor suppressor based on studies that it could inhibit cell transformation and has reduced expression in prostate and breast cancer.[13–15] Furthermore, ANP32A is a positive prognostic marker in non-small-cell lung cancer.[16] However, ANP32A was also shown to be upregulated in primary acute myeloid leukemia cells and promotes leukemogenesis.[17] ANP32E similarly shows enhanced expression in gastric cancer and is a negative prognostic marker in myeloma.[18,19] However, it is also reported that higher expression of ANP32E was associated with extended survival in follicular lymphoma.[20]

ANP32B is the most critical gene for normal development by comparing the effects of *Anp32b* deficiency to those of *Anp32a* or *Anp32e* deficiency in mice.[21] Previously, we showed that ANP32B acts as a negative regulator of leukemic cell apoptosis and a master enforcer of cell proliferation in breast cancer cells.[22,23] Recently, we also demonstrated that ANP32B-mediated repression of p53 maintains the function of chronic myelogenous leukemia (CML) stem cells and promotes CML progression.[24] Although it is ranked among the highest candidates in a tumor-suppressor-rich genome-wide search for recessive cancer genes,[25] the potential tumor-suppressor role of ANP32B remains largely unknown. Herein we investigate the function of ANP32B to B-ALL development using hematopoietic-specific *Anp32b* knockout mice and demonstrate that ANP32B suppresses B-ALL leukemogenesis by enhancing PU.1 activity.

2 | METHODS

2.1 | Mice

To delete the *Anp32b* gene specifically in the hematopoietic system, *Anp32b*$^{fl/fl}$ mice established at the Shanghai Model Organisms Center were crossed with *Scl-Cre* transgenic mice. All these strains were maintained on a C57BL/6 background. Six-week-old *Scl-Cre* mice were injected intraperitoneally daily with tamoxifen (10 mg/mL in corn oil; Sigma) at 50 μg/g body weight for 21 days to induce the *Scl-Cre* transgene. Genotyping primers are listed in Table S1. All of the animal experiments were conducted according to the Guideline for Animal Care at Shanghai Jiao Tong University School of Medicine.

2.2 | B-ALL mice model

To establish an N-myc-induced or BCR-ABL^{p190}-induced murine B-ALL, B220$^+$ cells were sorted from the bone marrow of 10–12-week-old donor mice, and infected with BCR-ABL^{p190}-GFP or N-myc-GFP retrovirus with polybrene (4 μg/mL). For transplantation, 1×10^5 B220$^+$ infected cells mixed with 2×10^5 competitor BM cells were directly injected through the tail vein into lethally irradiated C57BL/6 mice. For secondary transplantation, 2×10^5 GFP$^+$ cells were isolated and transplanted into irradiated C57BL/6 mice with 2×10^5 competitor BM cells.

2.3 | Flow cytometry

For flow cytometry analyses, BM cells were filtered through a 40-μm strainer to obtain a single-cell suspension. Peripheral blood (PB) cells were treated with ammonium chloride potassium lysis buffer to remove red blood cells. The cells were stained with indicated fluorochrome-conjugated antibodies following the manufacturer's instructions. The antibodies and dyes used are listed in Table S1.

2.4 | Immunoprecipitation and mass spectrometry analysis

Immunoprecipitation of endogenous proteins or Flag-tagged proteins and nano liquid chromatography with tandem mass spectrometry (LC–MS/MS) used to identify interacting proteins were performed as previously described.[26,27] All the antibodies used for immunoprecipitation are listed in Table S1. ANP32B-interacting proteins identified by mass spectrometry are listed in Table S3.

2.5 | Immunofluorescence

The details of immunofluorescence have been described previously.[28] The primary antibodies used are shown in Table S1.

2.6 | ChIP-qRT-PCR

Chromatin immunoprecipitation (ChIP) experiments were performed similarly to those described previously[24] and 2×10^7 *Anp32b*$^{+/+}$ and *Anp32b*$^{-/-}$ GFP$^+$ cells were performed per reaction. The purified ChIP DNA was quantified by qRT-PCR. The primers used are listed in Table S1.

2.7 | Quantification and statistical analysis

For comparison between two experimental groups or a specific pair in a multigroup, two-tailed unpaired Student's *t*-test was used, where error bars denote mean ± SEM. For comparison of cell growth curves, two-way ANOVA was used. For analysis of survival rates, a log-rank (Mantel-Cox) test was performed. All the differences were considered to be statistically significant if $P < 0.05$.

3 | RESULTS

3.1 | ANP32B is lowly expressed and predicts a better prognosis in human B-ALL

To investigate the expression of ANP32B in B-ALL, we first analyzed the mRNA expression level of ANP32B in three B-ALL patient cohorts (GSE13159, GSE28497, and GSE33315). Interestingly, we observed that ANP32B was expressed at a significantly lower level in B-ALL patients compared with normal controls (Figure 1A). To support this, we further analyzed ANP32B mRNA and protein levels in mononuclear cells from bone marrow of eight cases of primary adult patients with B-ALL together with samples from 10 cases of nonleukemic individuals as control, and the results demonstrated that both ANP32B mRNA and protein levels were also aberrantly downregulated in B-ALL patients (Figure 1B,C and Table S2). Notably, higher ANP32B expression was associated with longer overall survival (OS) in B-ALL patients according to the COG P9906 childhood B-ALL cohort (Figure 1D). Together, these data suggest that ANP32B might play an important role in B-ALL.

3.2 | Loss of *Anp32b* promotes N-myc-induced B-ALL development

To investigate the potential role of ANP32B in B-ALL development, we established the N-myc-induced B-ALL mouse model, which can be achieved by retrovirally introducing N-myc-IRES-GFP into B220$^+$ BM cells, followed by transplantation into lethally irradiated mice (Figure S1A). Three weeks after transplantation, the number of peripheral blood mononuclear cells (PBMC) and GFP$^+$ leukemic cells in PB and BM in mice transplanted with N-myc-transduced B220$^+$ BM cells were significantly higher than mice transplanted with empty vector cells (Figure S1B–D). All GFP$^+$ leukemic cells in BM mainly expressed B-cell markers (B220$^+$CD19$^+$) but not myeloid markers (Mac-1$^+$Gr-1$^+$), and these B cells were mainly undifferentiated B progenitor cells (B220$^+$CD43$^+$IgM$^-$) (Figure S1E). In addition, tumor-bearing mice also had enlarged lymph nodes and exhibited hepatosplenomegaly (Figure S1F,G).

B220$^+$ BM cells of tamoxifen treated *Scl-Cre*$^-$; *Anp32b*$^{fl/fl}$ and *Scl-Cre*$^+$; *Anp32b*$^{fl/fl}$ mice, which we previously reported and referred to as *Anp32b*$^{+/+}$ and *Anp32b*$^{-/-}$ mice,[24] were infected with N-myc-GFP retrovirus and then transplanted into lethally irradiated recipients. The results showed that *Anp32b* deficiency significantly increased the engraftment of GFP$^+$B220$^+$ B lymphoid leukemia cells in PB and BM of recipient mice (Figure 2A,B). Giemsa–Wright staining displayed a higher frequency of immature blast cells in BM (Figure 2C), together with more massive splenomegaly and enlarged lymph nodes (Figure 2D,E), and significantly increased leukemia infiltration in spleen and lymph nodes in recipients of *Anp32b*$^{-/-}$ cells (Figure 2F). In line with this, recipients of *Anp32b*$^{-/-}$ cells showed remarkably reduced survival times during primary and secondary transplantation (Figure 2G). To exclude the possibility that the enhanced homing ability contributes to the effects of *Anp32b* loss, GFP$^+$ B-ALL cells sorted from *Anp32b*$^{+/+}$ and *Anp32b*$^{-/-}$ recipients were injected into lethally irradiated mice, followed by detection of homed GFP$^+$ B-ALL cells in PB, spleen, and BM. No significant difference was detected between two groups 18 h after injection (Figure 2H). Taken together, our data indicate that *Anp32b* loss significantly promotes N-myc-induced B-ALL development.

3.3 | Loss of *Anp32b* promotes BCR-ABL^{p190}-induced B-ALL development

To further confirm the role of ANP32B in B-ALL development, we established another B-ALL mouse model generated by transplantation of BCR-ABL^{p190}-transduced B220$^+$ BM cells into lethally irradiated recipient mice,[29] which reflects the pathology of human disease since BCR-ABL^{p190} fusion gene accounts for 90% in pediatric Ph$^+$ B-ALL and 50%–80% in adult Ph$^+$ B-ALL (Figure S2A). Leukemic development was characterized by expansion of B lymphoid leukemic cells in PB and BM, frequent hind leg paralysis, moderate hepatosplenomegaly, and enlarged lymphoid organs of recipients (Figure S2B–G). Then B220$^+$ BM cells of *Anp32b*$^{+/+}$ and *Anp32b*$^{-/-}$ mice were infected with BCR-ABL^{p190} retrovirus and transplanted into lethally irradiated recipients. Similarly, recipients of *Anp32b*$^{-/-}$ BM cells developed B-ALL significantly faster than recipients of *Anp32b*$^{+/+}$ BM cells. The GFP$^+$ leukemic cells were largely increased in PB and BM of *Anp32b*$^{-/-}$ B-ALL mice (Figure 3A–C). *Anp32b* deficiency also exhibited more frequent hind leg paralysis, massive splenomegaly, and enlarged lymph nodes with more severe infiltration of leukemic cells compared with their wild-type counterparts (Figure 3D–F). Consistently, recipients of *Anp32b*$^{-/-}$ cells had markedly decreased survival during primary and secondary transplantation (Figure 3G). Furthermore, the number of colonies formed by *Anp32b*$^{-/-}$ B-ALL cells was significantly increased compared with

Anp32b$^{+/+}$ controls in the first plating, and this enhancement was even more impressive in the second plating (Figure 3H). Collectively, these data suggest that *Anp32b* deficiency significantly promotes BCR-ABL^{p190}-induced B-ALL development.

3.4 | ANP32B directly interacts with PU.1

ANP32B has been found to bind transcription factors (TFs) and modulate their activity.[24,30] To explore the potential ANP32B-interacting proteins in B cells, BaF3 cells (a murine pro-B-cell line) were transfected with empty vector or Flag-ANP32B, followed by affinity purification using anti-Flag antibody, and the precipitates were analyzed by LC–MS/MS. In total, we identified 259 ANP32B-interacting proteins in B cells including p53 (Figure S3A and Table S3). Our recent study reveals that ANP32B interacts with p53 to regulate hematopoiesis and CML leukemogenesis.[24] To determine whether ANP32B inhibits B-ALL development through regulating p53 activity, we used *Anp32b*$^{+/+}$*p53*$^{+/+}$, *Anp32b*$^{+/+}$*p53*$^{+/-}$, *Anp32b*$^{-/-}$*p53*$^{+/+}$, and *Anp32b*$^{-/-}$*p53*$^{+/-}$ mice in our pervious study to induce B-ALL. Survival analysis showed that although heterozygous *p53* loss in *Anp32b*$^{+/+}$ cells accelerated BCR-ABL^{p190}-induced leukemogenesis, *Anp32b*$^{-/-}$*p53*$^{+/-}$ mice presented similar survival compared with *Anp32b*$^{-/-}$*p53*$^{+/+}$ mice (Figure S3B), suggesting

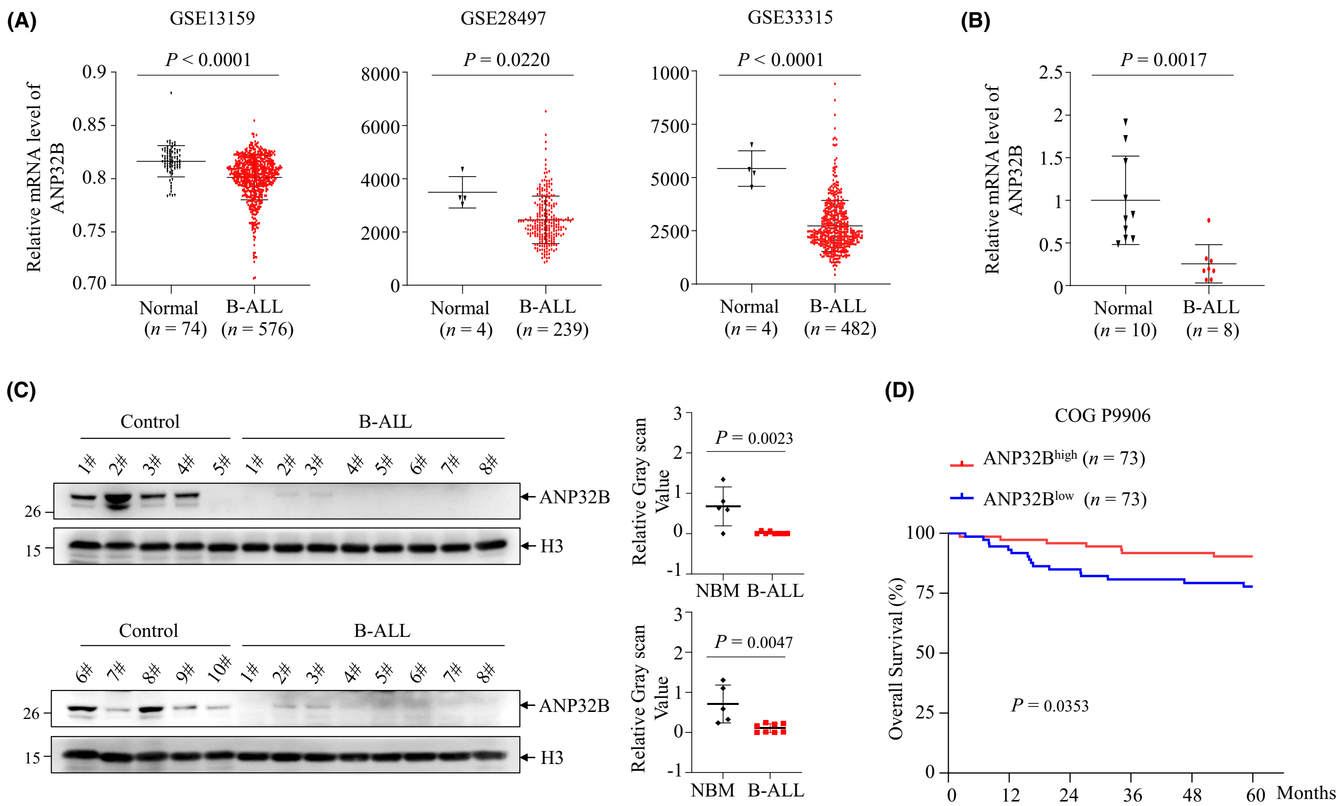

FIGURE 1 ANP32B is lowly expressed and predicts a better prognosis in B-ALL. (A) ANP32B mRNA expression level in B-ALL and normal bone marrow samples was analyzed in three published datasets. (B and C) Relative mRNA and protein expression levels of ANP32B in bone marrow mononuclear cells (BMMCs) of B-ALL and nonleukemic individuals were analyzed. (D) Overall survival of pediatric B-ALL patients from COG P9906 relative to ANP32B mRNA expression level.

FIGURE 2 Loss of *Anp32b* promotes N-myc-induced B-ALL development. (A) Flow cytometry plots (left) and statistics (right) of the percentage of GFP$^+$B220$^+$ cells in PB from recipients transplanted with N-myc-transduced *Anp32b*$^{+/+}$ and *Anp32b*$^{-/-}$ B220$^+$ BM cells ($n = 7$). (B) Flow cytometry plots (left) and statistics (right) of the percentage of GFP$^+$B220$^+$ cells in BM from recipients transplanted with N-myc-transduced *Anp32b*$^{+/+}$ and *Anp32b*$^{-/-}$ B220$^+$ BM cells ($n = 5$). (C) Representative images of Giemsa–Wright staining (left) for *Anp32b*$^{+/+}$ and *Anp32b*$^{-/-}$ BM cells on transplantation. Quantification of the percentage of blast cells is shown on the right ($n = 5$). Representative blast cells are indicated with red arrows. (D–F) Gross pathology of lymph nodes, spleens (D) and relative weights of the spleens (E), and hematoxylin–eosin staining of the spleens and lymph nodes (F) from recipients ($n = 5$). (G) Survival curves for recipients transplanted with N-myc-transduced *Anp32b*$^{+/+}$ and *Anp32b*$^{-/-}$ B220$^+$ BM cells on the first ($n = 5$) and second transplantation ($n = 4$). (H) Quantification of the frequencies of homed GFP$^+$ cells in PB, BM, and spleens in recipient mice receiving B-ALL cells 18 h after transplantation ($n = 5$). Error bars denote mean ± SEM. Statistical significance was determined by two-tailed unpaired *t*-test (A–C, E and H) or log-rank test (G) and the *P* values are shown. All animal experiments were repeated at least twice with similar results, and the results from one representative experiment are shown.

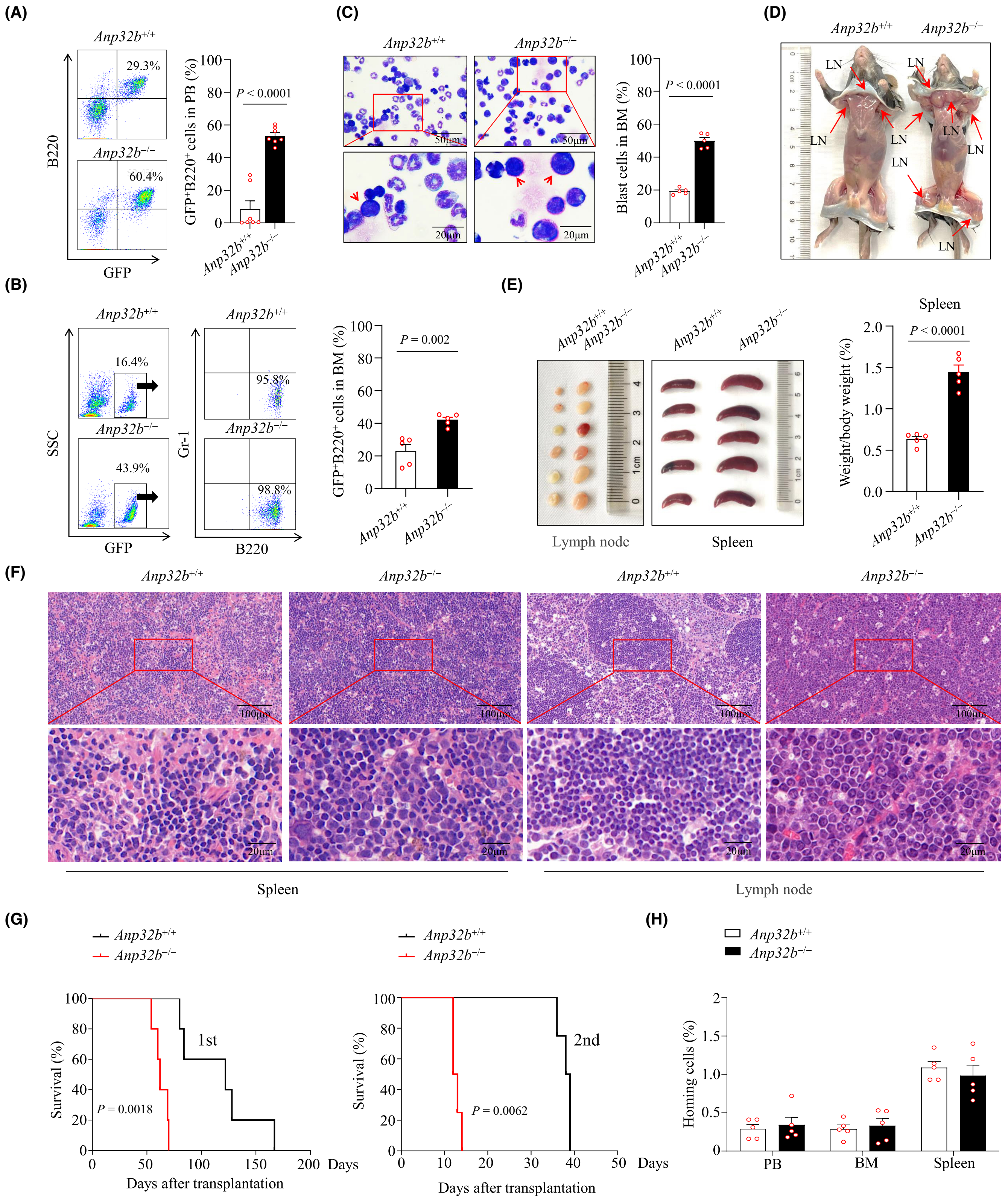

that *Anp32b*-deficiency promotes B-ALL development in a p53-independent manner.

In parallel, we performed RNA-seq analysis and revealed 393 significantly differentially expressed genes (DEGs) in *Anp32b*$^{-/-}$ B-ALL cells compared with the control ones. To further screen ANP32B-interacting transcriptional regulators, we compared the top 200 extracted upstream regulators through Ingenuity Pathway Analysis (IPA) with 259 ANP32B-interacting proteins and found an overlap of seven candidate genes (Figure S3A). Among these genes, only PU.1, a key regulator of B-cell fate specification,[31] was

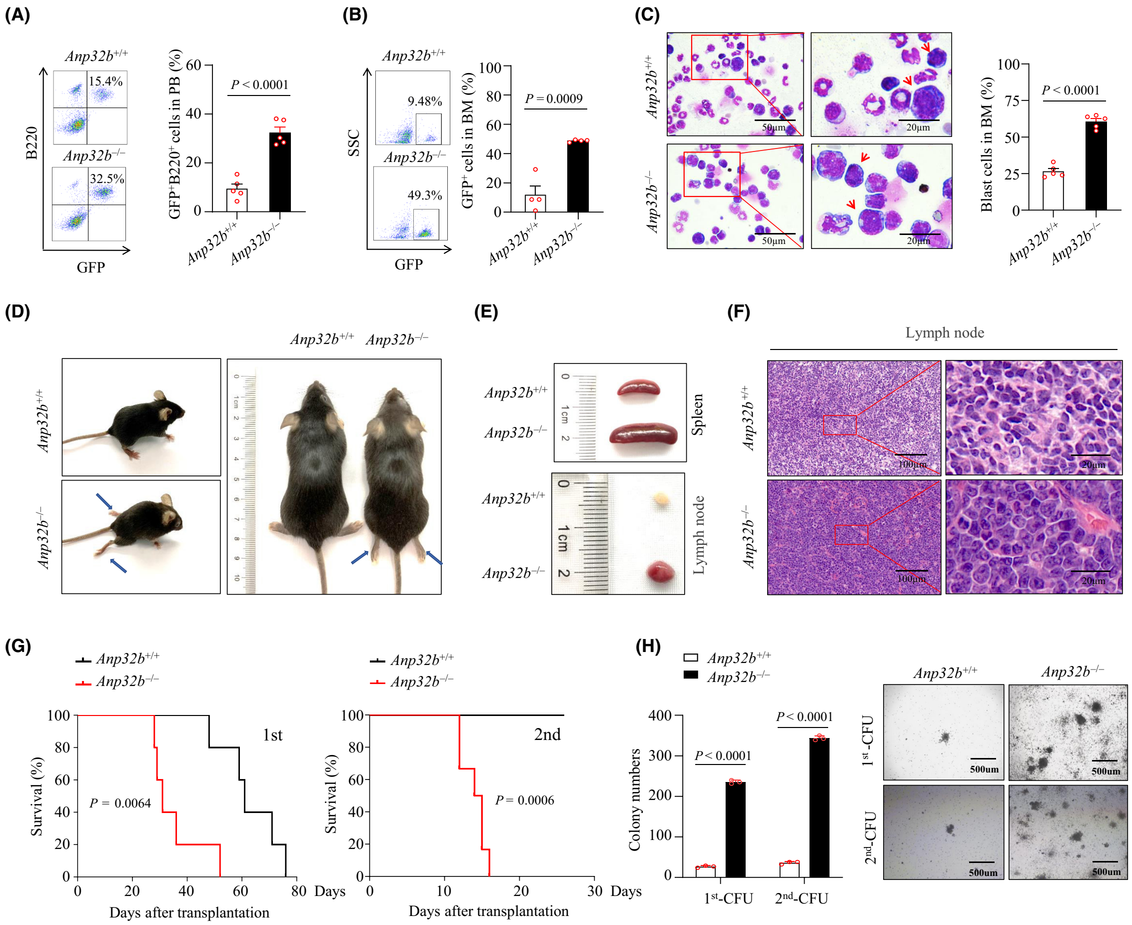

FIGURE 3 Loss of *Anp32b* promotes BCR-ABL^{p190}-induced B-ALL development. (A) Flow cytometry plots (left) and statistics (right) of the percentage of GFP$^+$B220$^+$ cells in PB from recipients receiving BCR-ABL^{p190}-transduced *Anp32b*$^{+/+}$ and *Anp32b*$^{-/-}$ B220$^+$ BM cells (*n* = 5). (B) Flow cytometry plots (left) and statistics (right) of the percentage of GFP$^+$ cells in BM from recipients receiving BCR-ABL^{p190}-transduced *Anp32b*$^{+/+}$ and *Anp32b*$^{-/-}$ B220$^+$ BM cells (*n* = 4). (C) Representative images of Giemsa–Wright staining (left) and frequencies of blast cells (right) for *Anp32b*$^{+/+}$ and *Anp32b*$^{-/-}$ BM cells on transplantation (*n* = 5). Representative blast cells are indicated with red arrows. (D) Gross appearance of *Anp32b*$^{+/+}$ and *Anp32b*$^{-/-}$ recipients. (E and F) Gross pathology of spleens, lymph nodes (E), and hematoxylin–eosin staining of lymph nodes (F) from recipients. (G) Survival curves for recipients transplanted with BCR-ABL^{p190}-transduced *Anp32b*$^{+/+}$ and *Anp32b*$^{-/-}$ B220$^+$ BM cells on the first (*n* = 5) and second transplantation (*n* = 6). (H) Primary and secondary colonies of GFP$^+$ cells sorted from the recipients receiving BCR-ABL^{p190}-transduced *Anp32b*$^{+/+}$ and *Anp32b*$^{-/-}$ B220$^+$ BM cells on first transplantation (*n* = 3). Error bars denote mean ± SEM. Statistical significance was determined by two-tailed unpaired *t*-test (A–C and H) or log-rank test (G) and the *P* values are shown. All animal experiments were repeated at least twice with similar results, and the results from one representative experiment are shown.

FIGURE 4 ANP32B interacts with PU.1 and enhances the transcriptional activity of PU.1. (A) Western blot analysis of indicated proteins in the inputs and immunoprecipitates of Flag-tagged ANP32B-transfected BaF3 cells. Empty vector (EV) serves as negative control. (B) Western blot analysis of indicated proteins in the inputs and immunoprecipitates of endogenous ANP32B in SEM cells. (C) Immunofluorescent staining of endogenous ANP32B, PU.1 together with re-staining of DAPI in Nalm6 cells followed by imaging with confocal microscopy. (D) Structure illustrations of full-length (FL) and fragments of PU.1 and ANP32B. (E) Western blot analysis of indicated proteins in the inputs and immunoprecipitates of anti-ANP32B antibody in 293T cells transfected with Flag-PU.1 full-length and its two fragments. (F) Western blot analysis of indicated proteins in the inputs and immunoprecipitates of anti-FLAG M2 beads in 293T cells transfected with Flag-ANP32B full-length and N163 segments. (G) Bacterially expressed ANP32B was incubated with GST or GST-tagged PU.1, GST-tagged PU.1 (170-270aa) followed by GST-tag pull down and Western blot analysis of indicated proteins. (H) GSEA analysis of RNA-seq data from recipients receiving N-myc-transduced *Anp32b*$^{+/+}$ and *Anp32b*$^{-/-}$ B220$^+$ BM cells using the PU.1-regulated gene set (GSE13125). (I and J) Clonally derived 293T cell lines depleted of ANP32B (gANP32B) or not (gNS), empty vector (EV), or Flag-ANP32B-infected 293T cells were co-transfected with PLVX-PU.1, luciferase reporter for PU.1 transcription (PU.1-luc), and Renilla luciferase reporter, and the relative luciferase activities were determined. (K) Relative mRNA expression levels of indicated genes in BM GFP$^+$ cells sorted from recipients receiving N-myc-transduced *Anp32b*$^{+/+}$ and *Anp32b*$^{-/-}$ B220$^+$ BM cells on first transplantation. (L) ChIP-quantitative RT-PCR of IgG and PU.1 on the promoters of the indicated genes in BM GFP$^+$ cells from recipients receiving N-myc-transduced *Anp32b*$^{+/+}$ and *Anp32b*$^{-/-}$ B220$^+$ BM cells. Error bars denote mean ± SEM. Statistical significance was determined by two-tailed unpaired *t*-test (I–L) and the *P* values are shown. The experiments in (A–G) and (I–L) were repeated three times independently with similar results.

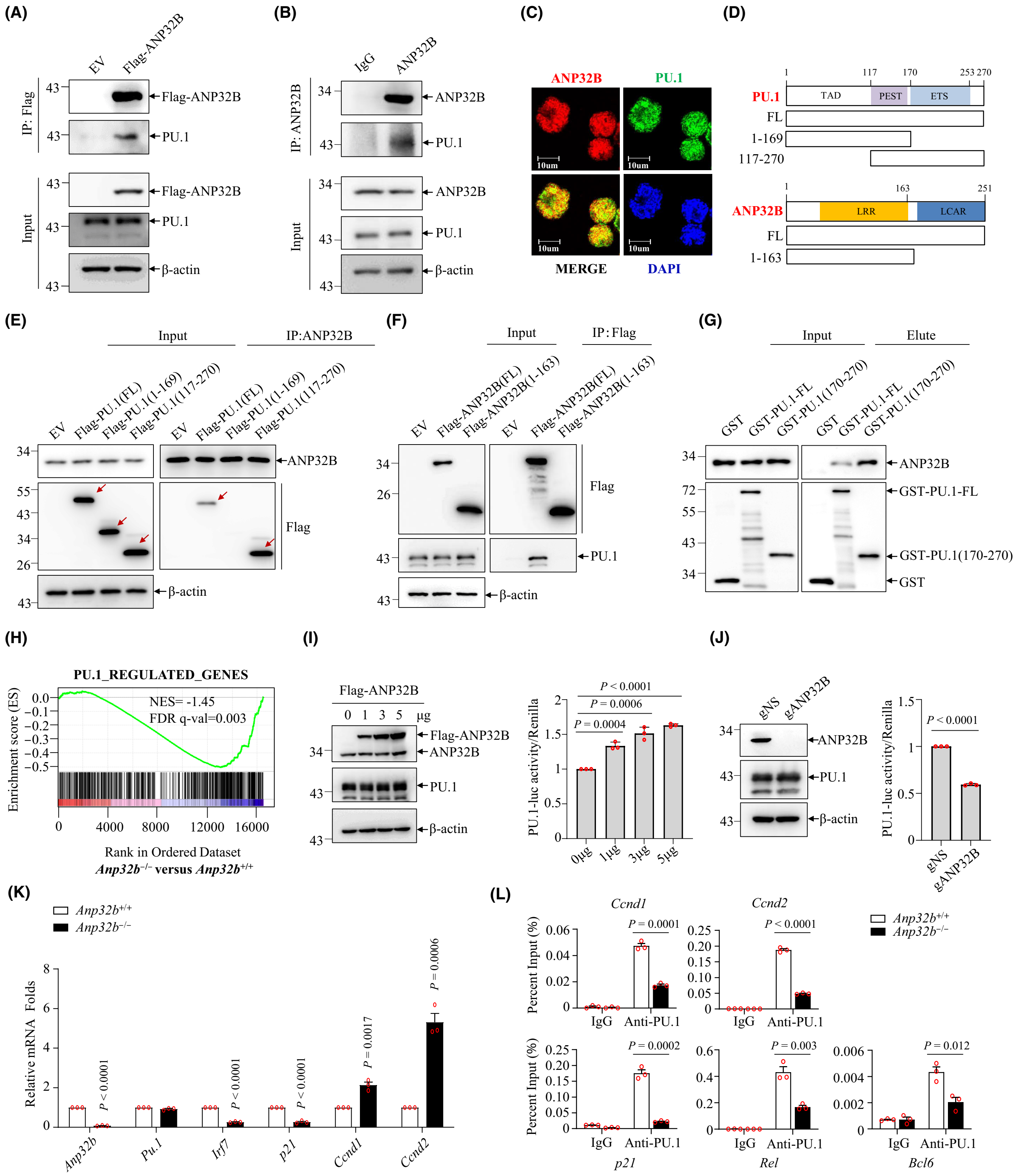

marked as a significantly inhibited regulator (z-score = −2.608) in the $Anp32b^{-/-}$ B-ALL group (Figure S3C), suggesting that ANP32B might interact with PU.1 and enhance its transcriptional activity.

We continued to investigate the relationship between ANP32B and PU.1. As shown in Figure 4A and Figure S3D, Flag-tagged ANP32B could immunoprecipitate endogenous PU.1 in mouse BaF3 and BaF3/BCR-ABL^{p190}-expression cells. Endogenous ANP32B-PU.1 interaction was also validated in human B-ALL cell line SEM and Nalm6 (Figure 4B,C). To define the domains of ANP32B and PU.1 required for their interaction, Flag-tagged full-length PU.1 (FL) and its two fragments, PU.1 (1-169aa, TAD+PEST), PU.1 (117-270aa, ETS+PEST) (Figure 4D), were transfected in 293T cells, followed by co-immunoprecipitation (IP) with ANP32B antibody. The results showed that ANP32B pulled down FL and the 117–270 fragment, suggesting that ETS (DNA-binding domain) of PU.1 is essential for its interaction with ANP32B (Figure 4E). On the other hand, the N-terminal (1-163aa) of ANP32B did not interact with PU.1 (Figure 4F). These data suggest that the DNA-binding domain of PU.1 is required for its interaction with the C-terminal acidic domain of ANP32B. Furthermore, in vitro GST-pull down assay showed that either GST-PU.1 (FL) or GST-PU.1 (170-270aa) pulled down ANP32B (Figure 4G), supporting a direct interaction of ANP32B with PU.1 protein.

3.5 | ANP32B enhances the transcriptional activity of PU.1 in B-ALL

The above observations prompted us to investigate how ANP32B regulates PU.1 function. After ruling out that *Anp32b* deficiency or overexpression did not change the mRNA and protein level of PU.1 in B-ALL cells (Figure S3E–G), we performed a gene set enrichment analysis (GSEA) to gain a global view of the transcriptome profile regulated by ANP32B. In line with our previous hypothesis, PU.1 target genes were significantly enriched in the transcriptome of *Anp32b*$^{+/+}$ B-ALL cells, suggesting that ANP32B may positively regulate the transcriptional activity of PU.1 (Figure 4H). To support this, a specific PU.1 responsive element (RE)-driven luciferase assay showed that the transcriptional activity of PU.1 was ANP32B dose dependently enhanced on ANP32B overexpression and reduced on ANP32B knockout in 293T cells (Figure 4I,J). Accordingly, the mRNA levels of PU.1-activated genes *Irf7* and *p21*[32–34] were downregulated, while PU.1-inhibited genes *Ccnd1* and *Ccnd2*[34–36] were upregulated in *Anp32b*$^{-/-}$ B-ALL cells (Figure 4K). Because ANP32B antibody is not suitable for ChIP assay, we performed ChIP-seq analyses using Flag antibody in BaF3 cells transfected with Flag-ANP32B and compared the results with PU.1 ChIP-seq data from GSE22178 in hematopoietic progenitor cells. We obtained 41,223 and 25,855 binding sites for ANP32B and PU.1, respectively. ANP32B showed a similar peak distribution pattern to PU.1, most frequently in the promoter regions, followed by intergenic regions and introns (Figure S4A), especially around the regions of the TSS (Figure S4B). Significantly, 9638 (38.6%) of the PU.1 peaks overlapped with ANP32B peaks (Figure S4C), including PU.1-activated *p21*, *Bcl6*, *Rel* and PU.1-inhibited *Ccnd1*,*Ccnd2* (Figure S4D–H).[34,36,37] The common peak annotations and gene list are listed in Table S4. Homer known motif analysis showed that the PU.1 binding sequence enriched in ANP32B, PU.1 and ANP32B/PU.1 common binding sites (Figure S4I). To assess whether ANP32B affects the chromatin occupancy of PU.1 in B-ALL cells, we conducted ChIP-qRT-PCR assays in *Anp32b*$^{+/+}$ and *Anp32b*$^{-/-}$ B-ALL cells to monitor whether PU.1 is recruited to the promoters of PU.1 targeted genes including *p21*, *Ccnd1*, *Ccnd2*, *Bcl6*, and *Rel*. Intriguingly, *Anp32b* depletion significantly abolished the binding of PU.1 to these target genes (Figure 4L). All these data indicated that ANP32B co-localizes with PU.1 on the genome and promotes the binding of PU.1 to target genes.

3.6 | PU.1 suppresses B-ALL progression

Several lines of evidence have demonstrated that PU.1 is a potent tumor suppressor for B cell malignancies including multiple myeloma (MM) and classical Hodgkin lymphoma (cHL).[32,33,38] Conditional double deletion of PU.1/Spi-B or PU.1/IRF4 or PU.1/IRF8 developed pre-B-ALL at high frequency.[39,40] In line with this, PU.1 exhibited a significantly lower expression level in B-ALL patients compared with normal controls in GSE13159 dataset (Figure 5A). To investigate the functional role of elevated PU.1 expression in B-ALL cells, we transfected Flag-PU.1 into Nalm6 and BaF3/BCR-ABL^{p190} cells and found that PU.1 overexpression significantly inhibited cell proliferation and clonogenicity in these two cells (Figure 5B–E). Furthermore, we introduced Flag-PU.1 by lentiviral Flag-PU.1-IRES-RFP plasmids in BM GFP^{+} cells collected from N-myc-induced B-ALL mice, followed by transplantation into irradiated recipient mice. Then, the GFP^{+}RFP^{+} B-ALL cells were sorted and injected into lethally irradiated mice (Figure 5F). Western blot analysis showed that PU.1 was highly expressed in GFP^{+}RFP^{+} B-ALL cells (Figure 5G). Indeed, PU.1 overexpression obviously decreased the frequencies of GFP^{+}RFP^{+} B-ALL cells in PB of recipient mice (Figure 5H). Meanwhile, we observed decreased spleen, liver, and lymph node size (Figure 5I), and extended survival times in PU.1 overexpression recipient mice (Figure 5J). Consequently, the mRNA levels of PU.1-activated genes *Irf7* and *p21* were upregulated, while PU.1-inhibited genes *Ccnd1* and *Ccnd2* were downregulated in PU.1 overexpression B-ALL cells (Figure 5K). Collectively, these data indicate that overexpression of PU.1 inhibits B-ALL progression.

FIGURE 5 Overexpression of PU.1 suppresses B-ALL progression. (A) PU.1 mRNA expression level in B-ALL and normal bone marrow samples was analyzed in GSE13159. (B) Western blot analysis of PU.1 expression in Nalm6 cells infected with EV and Flag-PU.1 (left). Cell numbers were counted on the indicated days (right, $n=3$). (C) Colony-forming assay for Nalm6 cells infected with EV or Flag-PU.1. Colony numbers were evaluated at day 7 ($n=3$). (D) Western blot analysis of BCR-ABL^{p190} and PU.1 expression in BaF3/BCR-ABL^{p190} cells infected with *EV* and *Flag-PU.1* (left). Cell numbers were counted at the indicated days (right, $n=3$). (E) Colony-forming assay for BaF3/BCR-ABL^{p190} cells infected with *EV* or *Flag-PU.1*. Colony numbers were evaluated at day 5 ($n=3$). (F) Schematic diagram evaluating the effect of PU.1 in the N-myc-induced B-ALL mice model. (G) Western blot analysis of indicated proteins in GFP^{+}RFP^{+} cells sorted from secondary recipients. (H) Flow cytometry plots (left) and statistics (right) of the percentage of GFP^{+}RFP^{+} cells in peripheral blood on secondary transplantation ($n=5$). (I) Gross pathology of the livers, spleens, and lymph nodes from the secondary recipients. (J) Survival curves for recipients receiving *EV* and *Flag-PU.1* GFP^{+}RFP^{+} cells on secondary transplantation ($n=6$). (K) Relative mRNA expression levels of indicated genes in GFP^{+}RFP^{+} BM cells sorted from *EV/Flag-PU.1* mice BM cells on secondary transplantation. Error bars denote mean ± SEM. Statistical significance was determined by two-tailed unpaired *t*-test (A, C, E, H, K), two-way ANOVA (B and D) or log-rank test (J) and the *P* values are shown. All animal experiments were repeated at least twice with similar results, and the results from one representative experiment are shown.

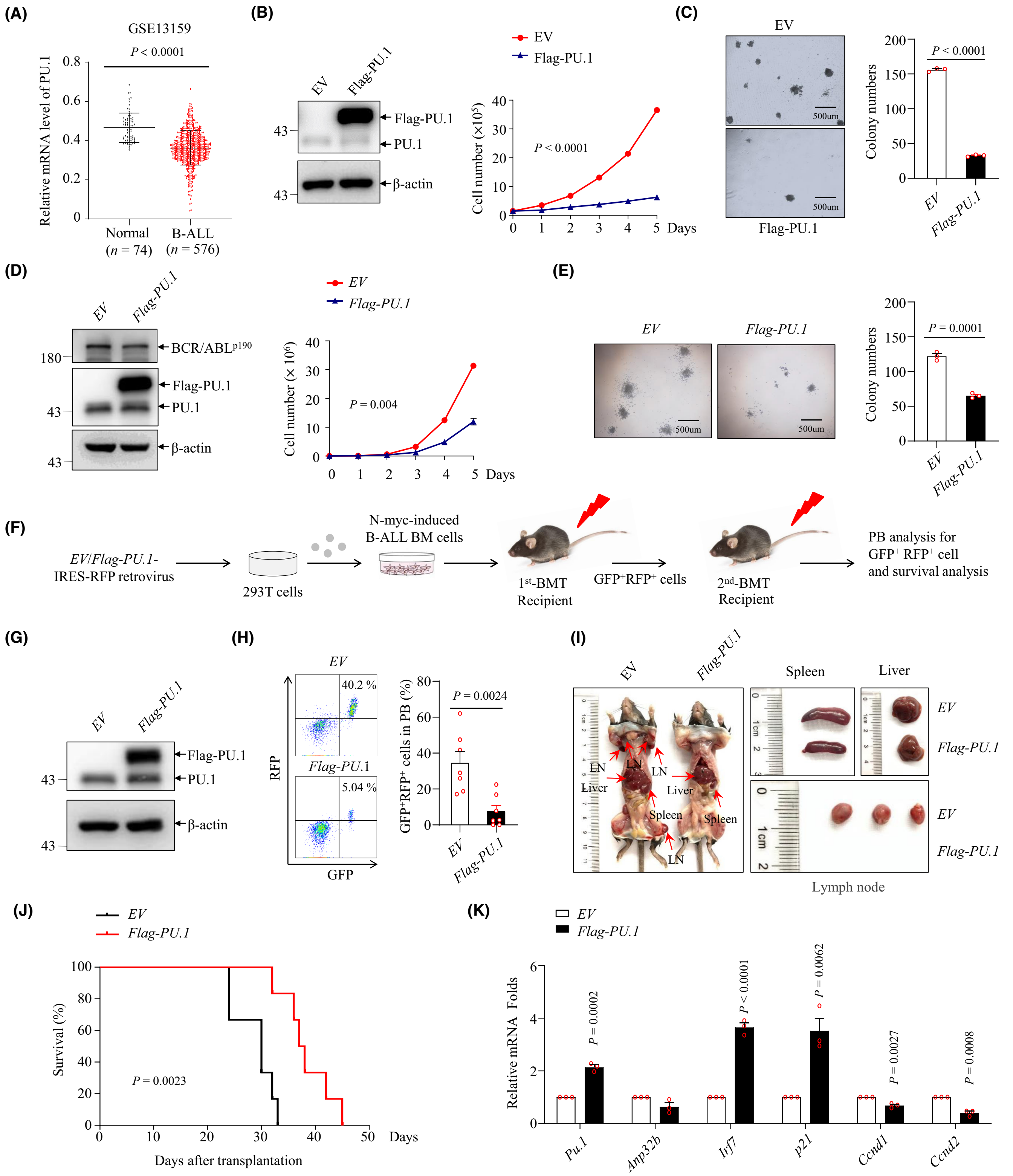

3.7 | PU.1 signaling rescues *Anp32b-deficiency* B-ALL phenotype

To confirm the requirement for PU.1 signaling for ANP32B-mediated B-ALL progression in vivo, we transfected XZ201-RFP-EV and XZ201-RFP-PU.1 into N-myc-induced *Anp32b*$^{+/+}$ and *Anp32b*$^{-/-}$ B-ALL cells, followed by transplantation into irradiated recipient mice. Then, the same number of GFP^{+}RFP^{+} B-ALL cells were sorted and injected into lethally irradiated mice. The mice transplanted with PU.1-overexpressed *Anp32b*$^{-/-}$ B-ALL cells presented extended survival compared with *Anp32b*$^{-/-}$ control mice, which was slightly inferior to *Anp32b*$^{+/+}$ mice (Figure 6A), suggesting PU.1 overexpression in *Anp32b*$^{-/-}$ B-ALL cells partially but significantly reversed accelerated leukemogenesis in *Anp32b*$^{-/-}$ mice.

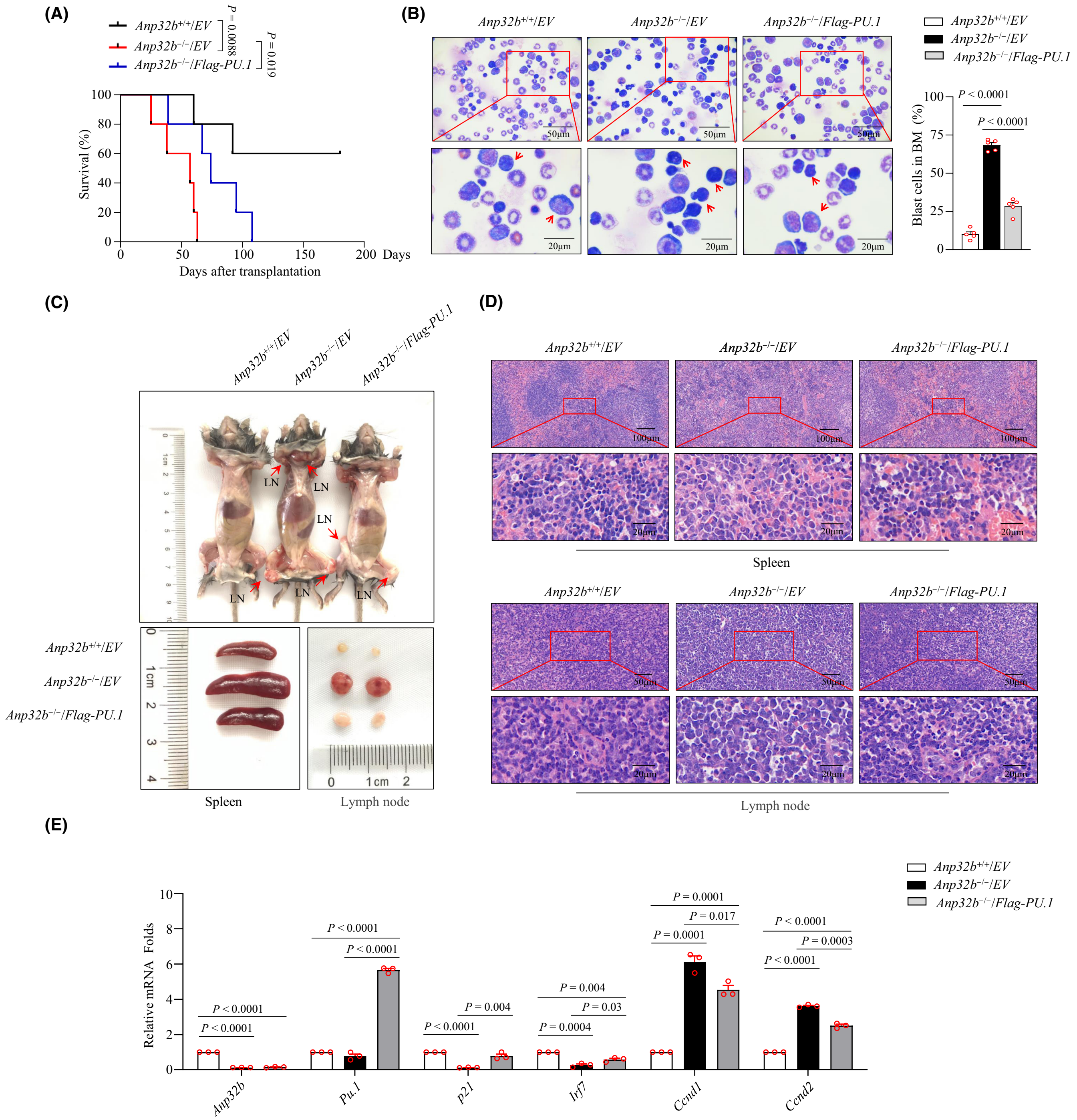

FIGURE 6 PU.1 signaling rescues the *Anp32b-deficiency* B-ALL phenotype. (A) Survival curves from secondary recipients injected with *Anp32b*$^{+/+}$*/EV*, *Anp32b*$^{-/-}$*/EV*, *Anp32b*$^{-/-}$*/Flag-PU.1* B-ALL cells ($n=5$). (B) Representative images of Giemsa–Wright staining for *Anp32b*$^{+/+}$*/EV*, *Anp32b*$^{-/-}$*/EV*, *Anp32b*$^{-/-}$*/Flag-PU.1* BM cells on second transplantation. Quantification of the frequencies of blast cells is shown on the right ($n=5$). Representative blast cells are indicated with red arrows. Gross pathology (C) and hematoxylin–eosin staining (D) of the spleens and lymph nodes from the secondary recipients. (E) Relative mRNA expression levels of indicated genes in GFP$^+$RFP$^+$ BM cells sorted from *Anp32b*$^{+/+}$*/EV*, *Anp32b*$^{-/-}$*/EV*, *Anp32b*$^{-/-}$*/Flag-PU.1* mice BM cells on secondary transplantation. Error bars denote mean ± SEM. Statistical significance was determined by two-tailed unpaired *t*-test (B and E) or log-rank test (A), and the *P* values are shown. All animal experiments were repeated at least twice with similar results, and the results of one representative experiment are shown.

Accordingly, the higher percentages of blast cells in BM, increased sizes of spleen/lymph nodes, and more severe tissue infiltration with leukemic cells in *Anp32b*$^{-/-}$ B-ALL mice were greatly rescued in PU.1-overexpressed *Anp32b*$^{-/-}$ B-ALL (Figure 6B–D). We sorted GFP$^+$RFP$^+$ BM cells from *Anp32b*$^{+/+}$*/EV*, *Anp32b*$^{-/-}$*/EV*, and *Anp32b*$^{-/-}$*/Flag-PU.1* mice and determined the mRNA level of PU.1 target genes by quantitative real-time polymerase chain reaction (Q-PCR). The mRNA levels of downregulated PU.1-activated genes *Irf7*, *p21* and upregulated PU.1-inhibited genes *Ccnd1*, *Ccnd2* in the *Anp32b*$^{-/-}$ B-ALL mice were rescued in PU.1 overexpressing *Anp32b* KO transformed cells (Figure 6E). All these data indicate that ANP32B enhances PU.1 activity to suppress B-ALL progression.

4 | DISCUSSION

The roles of ANP32B in tumorigenesis are due to its cellular and genetic context. Although ANP32B has been reported to serve as a tumor-promoting gene in breast cancer and CML,[23,24] to our knowledge this study provides the first evidence for the tumor-suppressive role of ANP32B in B-ALL. In contrast to high expression of ANP32B in CML patients compared with nonleukemic controls, ANP32B expression is inhibited in B-ALL patients through database analysis and clinical patient samples, and patients with low expression of ANP32B have poor prognostic outcome. DNA hypermethylation and post-translational regulation are common mechanisms for deregulation of tumor suppressor genes,[41,42] so the underlying mechanisms of down-regulation of ANP32B in B-ALL patients need to be further studied.

Substantial effort has been made to identify multiple key signaling pathways in B-ALL.[2,43] Mouse models provide invaluable tools for such studies, in part because they allow genetic manipulation of leukemic cells that is difficult to achieve using human cell lines or leukemia cells from patients. Here, we used two well-characterized mouse models to study the effect of *Anp32b* deficiency in B-ALL initiation and development. N-myc overexpression in committed progenitor B cells is able to induce pre-B-ALL/lymphoma.[44] The BCR-ABL^{p190}-induced mouse model is a human-relevant model reflecting the pathology of the human disease since human B-ALL cells usually contain a BCR-ABL^{p190} fusion gene.[45] Our results demonstrated that *Anp32b* deficiency significantly promotes B-ALL development in both models, suggesting that ANP32B has the same effect on different types of B-ALL driven by different gene mutants.

As a histone chaperone protein, ANP32B has been reported to form a repressive complex with p53 and KLF5, and thus inhibit their transcriptional activity.[24,30] After ruling out p53 signaling through which ANP32B regulates B-ALL progression, we further used combined proteomics and transcriptomics analysis to explore the potential ANP32B-interacting TFs in B cells. Interestingly, we found that ANP32B physically interacts with PU.1 and is recruited to the promotor of PU.1-targeted genes to enhance its transcription in B-ALL cells. Of note, ANP32B binds to the DNA-binding domain of PU.1, whereas binds to the C-terminal domain (CTD) of p53. The mechanisms of ANP32B acting as a coactivator for PU.1 or a corepressor for p53 need to be further addressed.

PU.1 plays crucial roles in the determination and differentiation of hematopoietic lineages,[46,47] and is associated with the occurrence of erythrocyte leukemia, pre-B-ALL, acute myeloid leukemia, and other diseases.[48–50] Here, we used cell lines and mouse models to demonstrate that PU.1 overexpression dramatically suppresses B-ALL progression, which is consistent with the tumor suppressor function in B-ALL revealed by *PU.1* and *Spi-B* double deletion. In particular, PU.1 overexpression in *Anp32b*-deficient B-ALL cells partially but significantly reversed accelerated leukemogenesis in *Anp32b* knockout mice, indicating that PU.1 is involved in the regulation of B-ALL progression by ANP32B. ANP32B is a well-known histone chaperone responsible for chromatin remodeling and epigenetic modification.[30,51] In this work, we identified seven candidate ANP32B-interacting proteins through LC–MS/MS combined IPA analysis. In addition, PU.1, histone deacetylase HDAC1, and chromatin remodeling gene SMARCA5 also play important roles in hematologic malignancies.[4,52–55] Whether or not these genes are involved in the accelerated B-ALL leukemogenesis caused by *Anp32b* deficiency deserves to be further explored. Given the cancer-promoting function of ANP32B in CML together with its tumor-suppressing role in B-ALL, we hypothesize that ANP32B is a "double-edged sword" in cancer progression. The diverse roles of ANP32B are likely due to the selective regulation of its binding TFs in different contexts. In summary, our results provide first evidence that ANP32B interacts with PU.1 and enhances its transcriptional activity, thereby suppressing B-ALL development in mice. Notably, ANP32B is lowly expressed in B-ALL patients, thus highlighting upregulation of ANP32B as a very promising therapeutic strategy for the treatment of B-ALL.

AUTHOR CONTRIBUTIONS

Q.Y., H.-R.L., and S.Y. performed most experiments. Y.-S.W., X.-N.Z., and Z.Z. conducted partial experiments. D.Z. provided clinical samples. Y.Y. and G.-Q.C. designed and supervised the entire project and prepared the manuscript.

ACKNOWLEDGMENTS

This work was supported by the National Key R&D Program of China (2020YFA0803403), the National Natural Science Foundation (91853206, 82270156) and its innovative group support (No. 81721004), the CAMS Innovation Fund for Medical Sciences (2019-I2M-5-051), and the Shanghai Committee of Science and Technology (20JC1410100).

CONFLICT OF INTEREST STATEMENT

The authors declare no conflict of interest.

ETHICAL APPROVAL

Approval of the Research Protocol by an Institutional Reviewer Board: N/A.

Informed Consent: N/A.

Registry and the Registration No. of the Study/Trial: N/A.

Animal Studies: All the animal experiments were approved by the Institutional Animal Care and Use Committee (IACUC) at Shanghai Jiao Tong University School of Medicine.

ORCID

Yun Yu https://orcid.org/0000-0001-6924-7456

REFERENCES

1. Loghavi S, Kutok JL, Jorgensen JL. B-acute lymphoblastic leukemia/lymphoblastic lymphoma. *Am J Clin Pathol*. 2015;144(3):393-410.
2. Roberts KG, Mullighan CG. Genomics in acute lymphoblastic leukaemia: insights and treatment implications. *Nat Rev Clin Oncol*. 2015;12(6):344-357.
3. Mullighan CG, Goorha S, Radtke I, et al. Genome-wide analysis of genetic alterations in acute lymphoblastic leukaemia. *Nature*. 2007;446(7137):758-764.
4. Stubbs MC, Kim W, Bariteau M, et al. Selective inhibition of HDAC1 and HDAC2 as a potential therapeutic option for B-ALL. *Clin Cancer Res*. 2015;21(10):2348-2358.
5. Iacobucci I, Mullighan CG. Genetic basis of acute lymphoblastic leukemia. *J Clin Oncol*. 2017;35(9):975-983.
6. Jabbour E, O'Brien S, Konopleva M, Kantarjian H. New insights into the pathophysiology and therapy of adult acute lymphoblastic leukemia. *Cancer*. 2015;121(15):2517-2528.
7. Park JH, Riviere I, Gonen M, et al. Long-term follow-up of CD19 CAR therapy in acute lymphoblastic leukemia. *N Engl J Med*. 2018;378(5):449-459.
8. Zhang Y, Zhang W, Dai H, et al. An analytical biomarker for treatment of patients with recurrent B-ALL after remission induced by infusion of anti-CD19 chimeric antigen receptor T (CAR-T) cells. *Sci China Life Sci*. 2016;59(4):379-385.
9. Maude SL, Teachey DT, Porter DL, Grupp SA. CD19-targeted chimeric antigen receptor T-cell therapy for acute lymphoblastic leukemia. *Blood*. 2015;125(26):4017-4023.
10. Dias A, Kenderian SJ, Westin GF, Litzow MR. Novel therapeutic strategies in acute lymphoblastic leukemia. *Curr Hematol Malig Rep*. 2016;11(4):253-264.
11. Matilla A, Radrizzani M. The Anp32 family of proteins containing leucine-rich repeats. *Cerebellum*. 2005;4(1):7-18.
12. Reilly PT, Yu Y, Hamiche A, Wang L. Cracking the ANP32 whips: important functions, unequal requirement, and hints at disease implications. *Bioessays*. 2014;36(11):1062-1071.
13. Kadkol SS, Brody JR, Pevsner J, Bai J, Pasternack GR. Modulation of oncogenic potential by alternative gene use in human prostate cancer. *Nat Med*. 1999;5(3):275-279.
14. Schafer ZT, Parrish AB, Wright KM, et al. Enhanced sensitivity to cytochrome c-induced apoptosis mediated by PHAPI in breast cancer cells. *Cancer Res*. 2006;66(4):2210-2218.
15. Pan W, da Graca LS, Shao Y, Yin Q, Wu H, Jiang X. PHAPI/pp32 suppresses tumorigenesis by stimulating apoptosis. *J Biol Chem*. 2009;284(11):6946-6954.
16. Hoffarth S, Zitzer A, Wiewrodt R, et al. pp32/PHAPI determines the apoptosis response of non-small-cell lung cancer. *Cell Death Differ*. 2008;15(1):161-170.
17. Yang X, Lu B, Sun X, et al. ANP32A regulates histone H3 acetylation and promotes leukemogenesis. *Leukemia*. 2018;32(7):1587-1597.
18. Tsukamoto Y, Uchida T, Karnan S, et al. Genome-wide analysis of DNA copy number alterations and gene expression in gastric cancer. *J Pathol*. 2008;216(4):471-482.
19. Walker BA, Leone PE, Chiecchio L, et al. A compendium of myeloma-associated chromosomal copy number abnormalities and their prognostic value. *Blood*. 2010;116(15):e56-e65.
20. Bjorck E, Ek S, Landgren O, et al. High expression of cyclin B1 predicts a favorable outcome in patients with follicular lymphoma. *Blood*. 2005;105(7):2908-2915.
21. Reilly PT, Afzal S, Gorrini C, et al. Acidic nuclear phosphoprotein 32kDa (ANP32)B-deficient mouse reveals a hierarchy of ANP32 importance in mammalian development. *Proc Natl Acad Sci USA*. 2011;108(25):10243-10248.
22. Shen SM, Yu Y, Wu YL, Cheng JK, Wang LS, Chen GQ. Downregulation of ANP32B, a novel substrate of caspase-3, enhances caspase-3 activation and apoptosis induction in myeloid leukemic cells. *Carcinogenesis*. 2010;31(3):419-426.
23. Yang S, Zhou L, Reilly PT, et al. ANP32B deficiency impairs proliferation and suppresses tumor progression by regulating AKT phosphorylation. *Cell Death Dis*. 2016;7:e2082.
24. Yang S, Zhu XN, Zhang HL, et al. ANP32B-mediated repression of p53 contributes to maintenance of normal and CML stem cells. *Blood*. 2021;138(24):2485-2498.
25. Volinia S, Mascellani N, Marchesini J, et al. Genome wide identification of recessive cancer genes by combinatorial mutation analysis. *PLoS One*. 2008;3(10):e3380.
26. Ge MK, Zhang N, Xia L, et al. FBXO22 degrades nuclear PTEN to promote tumorigenesis. *Nat Commun*. 2020;11(1):1720.
27. Shen SM, Zhang C, Ge MK, et al. PTENalpha and PTENbeta promote carcinogenesis through WDR5 and H3K4 trimethylation. *Nat Cell Biol*. 2019;21(11):1436-1448.
28. He P, Zhang C, Chen G, Shen S. Loss of lncRNA SNHG8 promotes epithelial-mesenchymal transition by destabilizing CDH1 mRNA. *Sci China Life Sci*. 2021;64(11):1858-1867.
29. Li S, Ilaria RL Jr, Million RP, Daley GQ, Van Etten RA. The P190, P210, and P230 forms of the BCR/ABL oncogene induce a similar chronic myeloid leukemia-like syndrome in mice but have different lymphoid leukemogenic activity. *J Exp Med*. 1999;189(9):1399-1412.
30. Munemasa Y, Suzuki T, Aizawa K, et al. Promoter region-specific histone incorporation by the novel histone chaperone ANP32B and DNA-binding factor KLF5. *Mol Cell Biol*. 2008;28(3):1171-1181.
31. Rosenbauer F, Owens BM, Yu L, et al. Lymphoid cell growth and transformation are suppressed by a key regulatory element of the gene encoding PU.1. *Nat Genet*. 2006;38(1):27-37.
32. Yuki H, Ueno S, Tatetsu H, et al. PU.1 is a potent tumor suppressor in classical Hodgkin lymphoma cells. *Blood*. 2013;121(6):962-970.
33. Ueno N, Nishimura N, Ueno S, et al. PU.1 acts as tumor suppressor for myeloma cells through direct transcriptional repression of IRF4. *Oncogene*. 2017;36(31):4481-4497.
34. Staber PB, Zhang P, Ye M, et al. Sustained PU.1 levels balance cell-cycle regulators to prevent exhaustion of adult hematopoietic stem cells. *Mol Cell*. 2013;49(5):934-946.
35. Vicari L, Eramo A, Manzella L, et al. The PU.1 transcription factor induces cyclin D2 expression in U937 cells. *Leukemia*. 2006;20(12):2208-2210.
36. Chavez JS, Rabe JL, Loeffler D, et al. PU.1 enforces quiescence and limits hematopoietic stem cell expansion during inflammatory stress. *J Exp Med*. 2021;218(6):e20201169.
37. Wang H, Jain S, Li P, et al. Transcription factors IRF8 and PU.1 are required for follicular B cell development and BCL6-driven germinal center responses. *Proc Natl Acad Sci USA*. 2019;116(19):9511-9520.
38. Tatetsu H, Ueno S, Hata H, et al. Down-regulation of PU.1 by methylation of distal regulatory elements and the promoter is required for myeloma cell growth. *Cancer Res*. 2007;67(11):5328-5336.
39. Pang SH, Minnich M, Gangatirkar P, et al. PU.1 cooperates with IRF4 and IRF8 to suppress pre-B-cell leukemia. *Leukemia*. 2016;30(6):1375-1387.
40. Xu LS, Sokalski KM, Hotke K, et al. Regulation of B cell linker protein transcription by PU.1 and Spi-B in murine B cell acute lymphoblastic leukemia. *J Immunol*. 2012;189(7):3347-3354.
41. Kulis M, Esteller M. DNA methylation and cancer. *Adv Genet*. 2010;70:27-56.
42. Chen L, Liu S, Tao Y. Regulating tumor suppressor genes: post-translational modifications. *Signal Transduct Target Ther*. 2020;5(1):90.

43. Hu Y, Yoshida T, Georgopoulos K. Transcriptional circuits in B cell transformation. *Curr Opin Hematol*. 2017;24(4):345-352.
44. Sugihara E, Shimizu T, Kojima K, et al. Ink4a and Arf are crucial factors in the determination of the cell of origin and the therapeutic sensitivity of Myc-induced mouse lymphoid tumor. *Oncogene*. 2012;31(23):2849-2861.
45. Chen C, Hao X, Lai X, et al. Oxidative phosphorylation enhances the leukemogenic capacity and resistance to chemotherapy of B cell acute lymphoblastic leukemia. *Sci Adv*. 2021;7(11):eabd6280.
46. Boasman K, Simmonds MJ, Graham C, Saunthararajah Y, Rinaldi CR. Using PU.1 and Jun dimerization protein 2 transcription factor expression in myelodysplastic syndromes to predict treatment response and leukaemia transformation. *Ann Hematol*. 2019;98(6):1529-1531.
47. Steidl U, Rosenbauer F, Verhaak RG, et al. Essential role of Jun family transcription factors in PU.1 knockdown-induced leukemic stem cells. *Nat Genet*. 2006;38(11):1269-1277.
48. Boddu P, Benton CB, Wang W, Borthakur G, Khoury JD, Pemmaraju N. Erythroleukemia-historical perspectives and recent advances in diagnosis and management. *Blood Rev*. 2018;32(2):96-105.
49. Takei H, Kobayashi SS. Targeting transcription factors in acute myeloid leukemia. *Int J Hematol*. 2019;109(1):28-34.
50. Batista CR, Lim M, Laramee AS, et al. Driver mutations in Janus kinases in a mouse model of B-cell leukemia induced by deletion of PU.1 and Spi-B. *Blood Adv*. 2018;2(21):2798-2810.
51. Tochio N, Umehara T, Munemasa Y, et al. Solution structure of histone chaperone ANP32B: interaction with core histones H3-H4 through its acidic concave domain. *J Mol Biol*. 2010;401(1):97-114.
52. Zikmund T, Paszekova H, Kokavec J, et al. Loss of ISWI ATPase SMARCA5 (SNF2H) in acute myeloid leukemia cells inhibits proliferation and chromatid cohesion. *Int J Mol Sci*. 2020;21(6):2073.
53. Stopka T, Zakova D, Fuchs O, et al. Chromatin remodeling gene SMARCA5 is dysregulated in primitive hematopoietic cells of acute leukemia. *Leukemia*. 2000;14(7):1247-1252.
54. Huang Y, Chen J, Lu C, et al. HDAC1 and Klf4 interplay critically regulates human myeloid leukemia cell proliferation. *Cell Death Dis*. 2014;5(10):e1491.
55. Santoro F, Botrugno OA, Dal Zuffo R, et al. A dual role for Hdac1: oncosuppressor in tumorigenesis, oncogene in tumor maintenance. *Blood*. 2013;121(17):3459-3468.

SUPPORTING INFORMATION

Additional supporting information can be found online in the Supporting Information section at the end of this article.

How to cite this article: Yang Q, Liu H-R, Yang S, et al. ANP32B suppresses B-cell acute lymphoblastic leukemia through activation of PU.1 in mice. *Cancer Sci*. 2023;114:2882-2894. doi:10.1111/cas.15822